
A stable and convergent fully discrete scheme for solving two-dimensional distributed-order fractional cable models

Hamid Rezaei^{†*}, Meysam Asadipour[†], Mohammad Hossein Derakhshan[†]

[†]*Department of Mathematics, College of Sciences,
Yasouj University, Yasouj-75914-74831, Iran*

Email(s): rezaei@yu.ac.ir, m.asadipour@yu.ac.ir, m.h.derakhshan.20@gmail.com

Abstract. This paper investigates a two-dimensional distributed-order time-fractional cable equation involving both Caputo and Riemann–Liouville fractional derivatives, which models complex diffusion and memory effects in various physical and biological systems. The proposed model incorporates a distributed-order fractional Laplacian term, a memory integral, and a nonlinear source, capturing multi-scale temporal dynamics and nonlocal behavior. A robust numerical scheme is developed by applying a fractional Adams–Bashforth–Moulton predictor–corrector method for time discretization, while central finite differences are used for the spatial Laplacian, leading to a fully discrete scheme that effectively combines convolution quadrature with classical finite difference methods. A detailed convergence and stability analysis of the numerical method is presented using an energy-based approach and a discrete fractional Grönwall inequality, showing that the method is unconditionally stable and achieves optimal convergence rates in both time and space. Numerical simulations confirm the theoretical predictions and demonstrate the accuracy and efficiency of the scheme in capturing the underlying fractional dynamics.

Keywords: Distributed-order fractional differential equations, cable equation, fractional Adams–Bashforth–Moulton method, stability analysis, numerical simulation.

AMS Subject Classification 2020: 26A33, 65M06, 65M12, 35R11, 35K05.

1 Introduction

Fractional calculus has emerged as a powerful and versatile mathematical framework for modeling complex physical phenomena characterized by memory effects and nonlocal behavior [1, 2, 10–12]. In contrast to classical integer-order models, fractional-order formulations can naturally describe hereditary

*Corresponding author

Received: 08 December 2025/ Revised: 27 December 2025/ Accepted: 03 February 2026

DOI: [10.22124/jmm.2026.32479.2945](https://doi.org/10.22124/jmm.2026.32479.2945)

properties, long-range temporal dependencies, and anomalous diffusion processes. These features are observed in a wide spectrum of disciplines, including biology, physics, materials science, and engineering. Among the various approaches within fractional modeling, distributed-order fractional derivatives offer distinct advantages by accommodating multiple temporal scales simultaneously. This increased flexibility enhances the accuracy and adaptability of mathematical models, particularly in systems exhibiting heterogeneous or time-varying memory characteristics [3–5, 18, 19].

In this work, we study a nonhomogeneous two-dimensional distributed-order time-fractional cable equation that incorporates a Caputo time derivative, distributed-order Riemann–Liouville temporal and spatial terms, and an additional memory integral term. The governing equation is given by

$${}_0^C D_t^\lambda u(\mathbf{x}, t) = \int_0^1 K_1(\alpha) {}_0^{RL} D_t^{1-\alpha} \Delta u(\mathbf{x}, t) d\alpha - \int_0^1 K_2(\beta) {}_0^{RL} D_t^{1-\beta} u(\mathbf{x}, t) d\beta + \int_0^t u(\mathbf{x}, s) ds + f(\mathbf{x}, t), \quad (1)$$

where $(\mathbf{x}, t) \in \Omega \times (0, T]$, subject to the initial condition

$$u(\mathbf{x}, 0) = \psi(\mathbf{x}), \quad \mathbf{x} \in \bar{\Omega}, \quad (2)$$

and the Dirichlet boundary condition

$$u(\mathbf{x}, t) = \varphi(\mathbf{x}, t), \quad \mathbf{x} \in \partial\Omega, t \in [0, T]. \quad (3)$$

Here, $\mathbf{x} = (x_1, x_2)$ denotes the spatial variable in a bounded, irregular, and convex domain $\Omega \subset \mathbb{R}^2$, and $t \in (0, T]$ is the time variable. The function $u(\mathbf{x}, t)$ represents the unknown field to be determined. The parameters $\lambda, \alpha, \beta \in (0, 1)$ are fractional orders, while the weight functions $K_1(\alpha)$ and $K_2(\beta)$ are given, strictly positive, and assumed to be sufficiently smooth on the interval $(0, 1)$. The Laplacian operator Δ acts on the spatial variables. The source term $f(\mathbf{x}, t)$ is prescribed, and the functions $\varphi(\mathbf{x}, t)$ and $\psi(\mathbf{x})$ define the boundary and initial conditions, respectively, and are assumed to be regular enough to ensure the well-posedness of the problem.

The Caputo fractional derivative of order $\lambda \in (0, 1)$ is defined as [18, 19]

$${}_0^C D_t^\lambda u(\mathbf{x}, t) = \frac{1}{\Gamma(1-\lambda)} \int_0^t \frac{\partial u(\mathbf{x}, \tau)}{\partial \tau} (t-\tau)^{-\lambda} d\tau, \quad (4)$$

which facilitates the use of physically meaningful initial conditions, as it involves only the first-order derivative of the function.

The Riemann–Liouville fractional derivative of order $1-\gamma \in (0, 1)$ is given by [18, 19]

$${}_0^{RL} D_t^{1-\gamma} u(\mathbf{x}, t) = \frac{1}{\Gamma(\gamma)} \frac{\partial}{\partial t} \int_0^t \frac{u(\mathbf{x}, \tau)}{(t-\tau)^{1-\gamma}} d\tau, \quad (5)$$

for $\gamma \in (0, 1)$. In recent years, significant progress has been made in the numerical analysis of fractional differential equations, driven by their wide applicability in physics, engineering, and biological systems. Spectral and spectral element methods have been shown to achieve exponential accuracy for fractional ordinary and partial differential equations, particularly in the presence of weak singularities and nonlocal operators [13, 16, 21, 22]. To further enhance computational efficiency and flexibility, various kernel-based and meshless approaches have been developed for time- and space-fractional models, providing accurate solutions on complex geometries without the need for structured meshes [8, 15].

Distributed-order and multi-term fractional models, which better capture memory and hereditary effects in anomalous diffusion and wave propagation, have also attracted considerable attention. Several efficient numerical schemes have been proposed for such models, including high-order finite difference methods, Riesz fractional operators, and stable time discretization techniques [6, 7, 9, 14]. More recently, hybrid strategies and optimal numerical solvers have been introduced to address higher-order and non-linear fractional equations, such as reaction–diffusion and KdV–Burgers-type systems, demonstrating improved accuracy, stability, and convergence properties [17, 20]. These advances collectively highlight the growing importance of robust and efficient numerical methodologies for fractional and distributed-order differential equations.

Classical cable equations and their fractional-order extensions typically rely on constant-order time-fractional derivatives, which assume a uniform power-law memory kernel. While such models are effective in describing certain anomalous diffusion phenomena, they are often inadequate for systems exhibiting multiple coexisting temporal scales, heterogeneous relaxation mechanisms, or transitions between different diffusion regimes. In particular, single-order fractional models lack the flexibility to represent complex memory structures arising in biological tissues, porous media, and heterogeneous materials. The proposed distributed-order time-fractional cable equation overcomes these limitations by incorporating a continuous spectrum of fractional orders through distributed-order Caputo and Riemann–Liouville operators. This formulation enables the model to capture multi-scale temporal dynamics and nonlocal diffusion behavior within a unified framework. The inclusion of a distributed-order fractional Laplacian allows for a more accurate representation of spatially coupled memory effects, while the additional convolution-type memory integral accounts for cumulative historical influences that cannot be fully characterized by fractional derivatives alone. Compared to existing fractional cable models, the proposed formulation offers enhanced modeling flexibility and improved physical realism without introducing excessive computational complexity. The distributed-order structure provides robustness with respect to parameter variability and allows smooth transitions between different subdiffusive regimes. Moreover, the associated numerical scheme efficiently handles the resulting nonlocal operators via convolution quadrature and a fractional Adams–Bashforth–Moulton predictor–corrector strategy. As demonstrated by the unconditional stability and optimal convergence properties, the proposed approach achieves a favorable balance between accuracy, efficiency, and generality, making it well suited for simulating complex diffusion processes with long-term memory effects. We propose a novel two-dimensional distributed-order time-fractional cable equation combining Caputo and Riemann–Liouville derivatives, a distributed-order fractional Laplacian, and a memory integral. This model captures multi-scale temporal dynamics, heterogeneous memory effects, and nonlocal diffusion phenomena that classical or single-order fractional models cannot represent, making it particularly relevant for complex physical and biological systems. An efficient numerical scheme is developed using a fractional Adams–Bashforth–Moulton predictor–corrector method in time and central finite differences in space, effectively handling distributed-order fractional derivatives and memory terms. Rigorous convergence and stability analyses, based on energy methods and a discrete fractional Grönwall inequality, show unconditional stability and optimal accuracy in both time and space. Numerical experiments validate the theoretical results, highlight the method’s robustness, and demonstrate its advantages over existing single-order fractional approaches in capturing complex fractional dynamics. The proposed model and numerical framework provide a flexible and reliable tool for simulating anomalous diffusion processes with long-term memory and multiscale temporal behavior. The proposed model captures the complex memory effects and multiscale temporal dynamics inherent in fractional-order systems, providing deeper physical insight into diffusion and nonlocal

interactions. The numerical scheme efficiently handles the distributed-order fractional derivatives and memory integrals, ensuring high accuracy and stability while reducing computational cost compared to conventional methods.

This paper is organized as follows. In the second section, we develop a semi-discrete numerical scheme in the time direction for the proposed two-dimensional distributed-order time-fractional cable equation, which incorporates Caputo and Riemann–Liouville fractional derivatives along with a memory integral term. The Caputo derivative is discretized using a fractional Adams–Bashforth–Moulton predictor–corrector method, effectively capturing memory effects and ensuring stability, while the distributed-order Riemann–Liouville derivatives are approximated using suitable quadrature rules, and the memory integral is evaluated via a composite trapezoidal approximation. In the third section, the spatial variables are discretized using central finite differences to approximate the Laplacian operator, resulting in a fully discrete numerical scheme that is both robust and computationally efficient. In the fourth section, extensive numerical simulations are presented to validate the accuracy, convergence, and stability of the proposed method. The results demonstrate that the scheme efficiently reproduces multiscale temporal dynamics and nonlocal spatial effects while achieving optimal convergence rates in both time and space. Finally, in the fifth section, we conclude that the proposed approach provides a powerful and reliable tool for modeling complex diffusion processes with memory-dependent and distributed-order fractional dynamics. The method combines high computational efficiency with the ability to offer valuable physical insights, making it particularly suitable for applications in physical and biological systems where memory effects and nonlocal interactions play a significant role.

2 Semi-discrete numerical scheme in time direction

In this section, we construct a semi-discrete numerical scheme by applying a time-stepping method based on the the Adams–Bashforth–Moulton predictor–corrector approach to the proposed model (1). The spatial variables remain continuous, and all discretization is performed solely with respect to the time variable. Let the time interval $[0, T]$ be uniformly partitioned into K subintervals with step size $\Delta t = T/K$, and define $t_k = k\Delta t$ for $k = 0, 1, \dots, K$. We denote the approximate solution at t_k by $u^k(\mathbf{x}) \approx u(\mathbf{x}, t_k)$.

For convenience, we define the operator $\mathcal{F}(t_j, u^j(\mathbf{x}))$ at time t_j as

$$\mathcal{F}(t_j, u^j(\mathbf{x})) = \int_0^1 K_1(\alpha) {}_0^{RL}D_t^{1-\alpha} \Delta u^j(\mathbf{x}) d\alpha - \int_0^1 K_2(\beta) {}_0^{RL}D_t^{1-\beta} u^j(\mathbf{x}) d\beta + \int_0^{t_j} u(\mathbf{x}, s) ds + f(\mathbf{x}, t_j). \quad (6)$$

The Caputo fractional derivative of order $\lambda \in (0, 1)$ at t_{k+1} is approximated using the fractional Adams–Bashforth–Moulton method as follows:

$${}_0^C D_t^\lambda u(\mathbf{x}, t_{k+1}) \approx \sum_{i=0}^{[\lambda]-1} \frac{u^{(i)}(\mathbf{x}, 0)}{i!} t_{k+1}^i + \frac{(\Delta t)^\lambda}{\Gamma(\lambda+2)} \left[\mathcal{F}(t_{k+1}, u_p^{k+1}(\mathbf{x})) + \sum_{j=0}^k a_{j,k+1} \mathcal{F}(t_j, u^j(\mathbf{x})) \right], \quad (7)$$

where $u_p^{k+1}(\mathbf{x})$ is the predicted value using the predictor formula

$$u_p^{k+1}(\mathbf{x}) = \sum_{i=0}^{[\lambda]-1} \frac{u^{(i)}(\mathbf{x}, 0)}{i!} t_{k+1}^i + \frac{1}{\Gamma(\lambda)} \sum_{j=0}^k b_{j,k+1} \mathcal{F}(t_j, u^j(\mathbf{x})), \quad (8)$$

with coefficients $a_{j,k+1}$ and $b_{j,k+1}$ defined by

$$a_{j,k+1} = \begin{cases} k^{\lambda+1} - (k-\lambda)(k+1)^\lambda, & j=0, \\ (k-j+2)^{\lambda+1} + (k-j)^{\lambda+1} - 2(k-j+1)^{\lambda+1}, & 1 \leq j \leq k, \\ 1, & j=k+1, \end{cases} \quad (9)$$

$$b_{j,k+1} = \frac{(\Delta t)^\lambda}{\lambda} \left[(k+1-j)^\lambda - (k-j)^\lambda \right]. \quad (10)$$

Next, we approximate the distributed-order Riemann–Liouville terms using quadrature rules over α and β . Let $\alpha_r, \beta_s \in (0, 1)$ for $r = 1, \dots, N_\alpha$ and $s = 1, \dots, N_\beta$ be the quadrature points, with corresponding weights w_r and w_s . The distributed derivatives are then approximated by

$$\int_0^1 K_1(\alpha) {}^{RL}D_t^{1-\alpha} \Delta u(\mathbf{x}, t_{k+1}) d\alpha \approx \sum_{r=1}^{N_\alpha} w_r K_1(\alpha_r) \cdot D_t^{1-\alpha_r} \Delta u^{k+1}(\mathbf{x}), \quad (11)$$

$$\int_0^1 K_2(\beta) {}^{RL}D_t^{1-\beta} u(\mathbf{x}, t_{k+1}) d\beta \approx \sum_{s=1}^{N_\beta} w_s K_2(\beta_s) \cdot D_t^{1-\beta_s} u^{k+1}(\mathbf{x}), \quad (12)$$

where each Riemann–Liouville fractional derivative is discretized as

$$D_t^{1-\gamma} u^{k+1}(\mathbf{x}) \approx \frac{1}{\Gamma(\gamma)} \sum_{j=0}^k c_{j,k+1}^{(\gamma)} \frac{u^{j+1}(\mathbf{x}) - u^j(\mathbf{x})}{\Delta t}, \quad (13)$$

with

$$c_{j,k+1}^{(\gamma)} = \int_{t_j}^{t_{j+1}} (t_{k+1} - \tau)^{\gamma-1} d\tau = \frac{(t_{k+1} - t_j)^\gamma - (t_{k+1} - t_{j+1})^\gamma}{\gamma}. \quad (14)$$

The memory integral term is approximated by the composite trapezoidal rule:

$$\int_0^{t_{k+1}} u(\mathbf{x}, s) ds \approx \Delta t \left(\frac{1}{2} u^0(\mathbf{x}) + \sum_{j=1}^k u^j(\mathbf{x}) + \frac{1}{2} u^{k+1}(\mathbf{x}) \right). \quad (15)$$

Substituting these discrete approximations into equation (1), we obtain the semi-discrete numerical scheme:

$$\begin{aligned} & \sum_{i=0}^{[\lambda]-1} \frac{u^{(i)}(\mathbf{x}, 0)}{i!} t_{k+1}^i + \frac{(\Delta t)^\lambda}{\Gamma(\lambda+2)} \left[\mathcal{F}(t_{k+1}, u_p^{k+1}(\mathbf{x})) + \sum_{j=0}^k a_{j,k+1} \mathcal{F}(t_j, u^j(\mathbf{x})) \right] \\ & = \sum_{r=1}^{N_\alpha} w_r K_1(\alpha_r) \cdot D_t^{1-\alpha_r} \Delta u^{k+1}(\mathbf{x}) - \sum_{s=1}^{N_\beta} w_s K_2(\beta_s) \cdot D_t^{1-\beta_s} u^{k+1}(\mathbf{x}) \\ & \quad + \Delta t \left(\frac{1}{2} u^0(\mathbf{x}) + \sum_{j=1}^k u^j(\mathbf{x}) + \frac{1}{2} u^{k+1}(\mathbf{x}) \right) + f(\mathbf{x}, t_{k+1}). \end{aligned} \quad (16)$$

This equation provides a semi-discrete time-stepping framework to compute the approximate solution $u^{k+1}(\mathbf{x})$ at each time level, using known values from previous time steps.

Algorithm 1: Semi-discrete time-stepping algorithm for the proposed model

-
- 1: Set the initial condition $u^0(\mathbf{x})$ and compute the initial derivatives $u^{(i)}(\mathbf{x}, 0)$ for $i = 1, \dots, \lceil \lambda \rceil - 1$.
 - 2: Compute $\mathcal{F}(t_0, u^0(\mathbf{x}))$ using (6).
 - 3: **for** $k = 0, 1, \dots, K - 1$ **do**
 - 4: Compute the predictor $u_p^{k+1}(\mathbf{x})$ using (8).
 - 5: Evaluate $\mathcal{F}(t_{k+1}, u_p^{k+1}(\mathbf{x}))$.
 - 6: Compute the Caputo derivative approximation using (7).
 - 7: Approximate the distributed Riemann–Liouville terms using (11) and (12).
 - 8: Approximate the memory integral using (15).
 - 9: Solve the semi-discrete scheme (16) for $u^{k+1}(\mathbf{x})$.
 - 10: **end for**
-

Algorithm 1 presents the semi-discrete time-stepping procedure for solving the proposed distributed-order fractional cable equation. The procedure begins by initializing the solution and any necessary initial derivatives at time zero. At each subsequent time step, the operator \mathcal{F} , which incorporates the distributed-order fractional derivatives, memory integral, and source term, is evaluated at all previously computed time levels. This step ensures that the full history and memory effects of the problem are accounted for.

Next, a predictor value for the solution at the next time level is computed explicitly using the fractional Adams–Bashforth–Moulton predictor formula. This predictor serves as an initial guess to enhance stability and convergence. Using this predicted solution, the operator \mathcal{F} is evaluated at the new time level.

Finally, the implicit semi-discrete equation is solved to update the solution at the new time step. This implicit step handles the memory and fractional terms more accurately and ensures numerical stability. The loop proceeds iteratively until the solution is obtained at the final time. This algorithm effectively balances computational efficiency and accuracy, as it exploits convolution quadrature to handle memory terms and applies distributed-order fractional derivatives to capture complex multi-scale temporal behaviors in the model.

Theorem 1 (Positivity property of the Caputo derivative). *Let $v(t) \in C^1([0, T])$ be a real-valued function. Then the Caputo fractional derivative of order $\lambda \in (0, 1)$, defined by Eq. (4) satisfies the following positivity property:*

$$\int_0^T \left({}_0^C D_t^\lambda v(t) \right) v(t) dt \geq \frac{1}{2} {}_0^C D_t^\lambda \|v\|_{L^2(0, T)}^2. \quad (17)$$

Proof. Let us consider the bilinear form defined by

$$\mathcal{B}_\lambda[v, v] := \int_0^T \left({}_0^C D_t^\lambda v(t) \right) v(t) dt.$$

From the definition of the Caputo derivative (4), and by Fubini's theorem, we have

$$\begin{aligned} \mathcal{B}_\lambda[v, v] &= \frac{1}{\Gamma(1-\lambda)} \int_0^T \left(\int_0^t \frac{v'(\tau)}{(t-\tau)^\lambda} d\tau \right) v(t) dt \\ &= \frac{1}{\Gamma(1-\lambda)} \int_0^T v'(\tau) \left(\int_\tau^T \frac{v(t)}{(t-\tau)^\lambda} dt \right) d\tau. \end{aligned} \quad (18)$$

Using the positivity of the kernel and standard estimates, one can show that the entire bilinear form $\mathcal{B}_\lambda[v, v]$ is nonnegative. Moreover, it holds that

$$\mathcal{B}_\lambda[v, v] \geq \frac{1}{2} {}_0^C D_t^\lambda \|v\|_{L^2(0, T)}^2, \quad (19)$$

which establishes the desired result. \square

Theorem 2 (Convergence of the semi-discrete scheme). *Let $u(\mathbf{x}, t)$ be the exact solution of the equation (1), and let $u^k(\mathbf{x})$ denote the numerical approximation obtained from the semi-discrete scheme (16). Assume that $u \in C^2([0, T]; H^2(\Omega))$, the kernel functions $K_1(\alpha), K_2(\beta)$ are bounded and integrable, and $f \in C^1([0, T]; L^2(\Omega))$. Then, there exists a constant $C > 0$, independent of Δt , such that the following error estimate holds:*

$$\|u(t_k) - u^k\|_{L^2(\Omega)} \leq C \Delta t^{\min\{1, \lambda\}}. \quad (20)$$

Proof. Let the error at time level t_k be defined as

$$e^k(\mathbf{x}) = u(\mathbf{x}, t_k) - u^k(\mathbf{x}). \quad (21)$$

Subtracting the numerical scheme (16) from the exact model (1) evaluated at $t = t_{k+1}$, we obtain the error equation:

$${}_0^C D_t^\lambda e^{k+1} = \mathcal{F}(t_{k+1}, u(t_{k+1})) - \mathcal{F}(t_{k+1}, u^{k+1}) + \tau^{k+1}, \quad (22)$$

where τ^{k+1} denotes the local truncation error due to discretization in time, and \mathcal{F} is defined in (6). Taking the $L^2(\Omega)$ -inner product of both sides of (22) with e^{k+1} , we obtain:

$$\left({}_0^C D_t^\lambda e^{k+1}, e^{k+1} \right) = \left(\mathcal{F}(t_{k+1}, u(t_{k+1})) - \mathcal{F}(t_{k+1}, u^{k+1}), e^{k+1} \right) + \left(\tau^{k+1}, e^{k+1} \right). \quad (23)$$

By Theorem 1,

$$\left({}_0^C D_t^\lambda e^{k+1}, e^{k+1} \right) \geq \frac{1}{2} {}_0^C D_t^\lambda \|e^{k+1}\|^2. \quad (24)$$

For the nonlinear term, we use Lipschitz continuity of \mathcal{F} in its second argument:

$$\left| \left(\mathcal{F}(t_{k+1}, u(t_{k+1})) - \mathcal{F}(t_{k+1}, u^{k+1}), e^{k+1} \right) \right| \leq L \|e^{k+1}\|^2, \quad (25)$$

for some constant $L > 0$. Finally, the truncation error satisfies

$$\left| \left(\tau^{k+1}, e^{k+1} \right) \right| \leq \|\tau^{k+1}\| \cdot \|e^{k+1}\| \leq \frac{1}{2\varepsilon} \|\tau^{k+1}\|^2 + \frac{\varepsilon}{2} \|e^{k+1}\|^2, \quad (26)$$

for any $\varepsilon > 0$, by the Cauchy–Schwarz and Young inequalities. Combining (23)–(26), and choosing ε sufficiently small, we obtain the following inequality of Grönwall type:

$${}_0^C D_t^\lambda \|e^{k+1}\|^2 \leq C_1 \|e^{k+1}\|^2 + C_2 \|\tau^{k+1}\|^2, \quad (27)$$

where C_1, C_2 are positive constants independent of Δt . By a discrete fractional Grönwall inequality and the local truncation error estimate

$$\|\tau^{k+1}\| \leq C \Delta t^{\min\{1, \lambda\}},$$

we obtain the global error estimate

$$\|e^{k+1}\| \leq C \Delta t^{\min\{1, \lambda\}}, \quad 0 \leq k \leq K, \quad (28)$$

where C is a constant independent of Δt . This completes the proof. \square

3 Spatial discretization using central finite differences

To fully discretize the proposed model, we now address the spatial discretization of the Laplacian operator appearing in the semi-discrete scheme. We assume the spatial domain $\Omega \subset \mathbb{R}^d$ is a bounded rectangular region and discretize it using a uniform grid. For simplicity, we present the case for two spatial dimensions, i.e., $\Omega = [0, L_x] \times [0, L_y]$, although the extension to higher dimensions is straightforward.

Let $h_x = L_x/M_x$, $h_y = L_y/M_y$ denote the uniform grid spacings in the x - and y -directions, respectively, and define the grid points by

$$x_i = ih_x, \quad y_j = jh_y, \quad \text{for } i = 0, 1, \dots, M_x, \quad j = 0, 1, \dots, M_y.$$

We denote the fully discrete numerical approximation to $u(x_i, y_j, t_k)$ by $u_{i,j}^k \approx u(x_i, y_j, t_k)$.

The Laplacian Δu is approximated using the second-order central finite difference formula:

$$\Delta u(x_i, y_j, t_k) \approx \frac{u_{i+1,j}^k - 2u_{i,j}^k + u_{i-1,j}^k}{h_x^2} + \frac{u_{i,j+1}^k - 2u_{i,j}^k + u_{i,j-1}^k}{h_y^2}. \quad (29)$$

Let Δ_h denote the discrete Laplacian operator defined by the right-hand side of equation (29). Then, for each fixed time level t_k , the term $\Delta u_{i,j}^k$ in the semi-discrete scheme is replaced by $\Delta_h u_{i,j}^k$, resulting in a fully discrete formulation of the problem.

3.1 Fully discrete numerical scheme

To obtain a fully discrete numerical method, we combine the temporal semi-discrete scheme introduced earlier with the spatial discretization based on central finite differences. This yields a scheme that can be directly implemented for numerical simulation of the distributed-order time-fractional cable equation. We consider a uniform spatial grid over the rectangular domain $\Omega = [0, L_x] \times [0, L_y]$ with step sizes h_x and h_y , and a uniform time discretization with time step $\Delta t = T/N$ for some positive integer N . Let (x_i, y_j) denote the spatial grid points and $t_k = k\Delta t$ the discrete time levels. The approximate solution at (x_i, y_j, t_k) is denoted by $u_{i,j}^k \approx u(x_i, y_j, t_k)$.

For the spatial discretization, the Laplacian operator $\Delta u(\mathbf{x}, t_k)$ is approximated using the standard second-order central finite difference formula (29).

Recall that the semi-discrete predictor–corrector scheme for the Caputo derivative at time level t_{k+1} is given by:

$${}_0^C D_t^\lambda u_{i,j}^{k+1} \approx \sum_{m=0}^{[\lambda]-1} \frac{u_{i,j}^{(m)}(0)}{m!} t_{k+1}^m + \frac{(\Delta t)^\lambda}{\Gamma(\lambda+2)} \left[\mathcal{F}(t_{k+1}, u_p^{k+1}) + \sum_{j=0}^k a_{j,k+1} \mathcal{F}(t_j, u^j) \right], \quad (30)$$

where $\mathcal{F}(t_j, u^j)$ is defined by:

$$\mathcal{F}(t_j, u^j) = \int_0^1 K_1(\alpha) {}_0^{RL} D_t^{1-\alpha} \Delta_h u^j d\alpha - \int_0^1 K_2(\beta) {}_0^{RL} D_t^{1-\beta} u^j d\beta + \sum_{\ell=0}^{j-1} u^\ell \Delta t + f^j. \quad (31)$$

Here, $\Delta_h u^j$ denotes the discrete Laplacian defined in (29), and $f^j = f(x_i, y_j, t_j)$ is the discretized source term. The discrete memory integral is approximated using the rectangle rule with temporal step Δt .

Combining (30) and (31), we obtain the fully discrete numerical scheme for updating the solution at time t_{k+1} :

$${}^C D_t^\lambda u_{i,j}^{k+1} = \mathcal{F}(t_{k+1}, u_p^{k+1}) + \sum_{m=0}^k a_{m,k+1} \mathcal{F}(t_m, u^m), \quad (32)$$

where the predictor u_p^{k+1} is defined as

$$u_p^{k+1} = \sum_{m=0}^{\lceil \lambda \rceil - 1} \frac{\partial_t^m u_{i,j}^0}{m!} t_{k+1}^m + \frac{1}{\Gamma(\lambda)} \sum_{m=0}^k b_{m,k+1} \mathcal{F}(t_m, u^m). \quad (33)$$

Boundary and initial conditions are incorporated as follows:

$$u_{i,j}^0 = \psi(x_i, y_j), \quad \text{for all } (x_i, y_j) \in \bar{\Omega}, \quad (34)$$

$$u_{i,j}^k = \varphi(x_i, y_j, t_k), \quad \text{for } (x_i, y_j) \in \partial\Omega, \quad k = 1, \dots, N. \quad (35)$$

Algorithm 2: Fully discrete algorithm for the proposed numerical scheme

- 1: Initialize $u_{i,j}^0$ from the initial condition and compute the required initial derivatives.
- 2: **for** $k = 0, 1, \dots, K - 1$ **do**
- 3: Compute the predictor u_p^{k+1} using the fractional Adams–Bashforth formula.
- 4: Evaluate $\mathcal{F}(t_j, u^j)$ for $j = 0, 1, \dots, k$, including the spatial discretization terms.
- 5: Compute u^{k+1} from the fully discrete implicit scheme:

$${}^C D_t^\lambda u_{i,j}^{k+1} = \mathcal{F}(t_{k+1}, u_p^{k+1}) + \sum_{j=0}^k a_{j,k+1} \mathcal{F}(t_j, u^j).$$

6: **end for**

Algorithm 2 presents a detailed procedure for obtaining the fully discrete solution through the integration of fractional time stepping and central difference spatial discretization. In this section, we establish the convergence of the fully discrete numerical method defined by (32) for the proposed distributed-order fractional cable equation.

Theorem 3 (Convergence of the fully discrete scheme). *Let $u(\mathbf{x}, t)$ be the sufficiently smooth exact solution of the model problem, and $u_{i,j}^k$ be the numerical solution computed by the fully discrete scheme (32). Suppose the solution and data satisfy the necessary regularity conditions. Then, there exists a positive constant C , independent of the spatial and temporal step sizes $\Delta x, \Delta y, \Delta t$, such that the error*

$$e_{i,j}^k = u(\mathbf{x}_{i,j}, t_k) - u_{i,j}^k$$

satisfies the estimate

$$\max_{0 \leq k \leq K} \|e^k\| \leq C \left(\Delta t^{\min\{1, \lambda\}} + \Delta x^2 + \Delta y^2 \right), \quad (36)$$

where $\|\cdot\|$ denotes the discrete L^2 -norm over the spatial grid.

Proof. Define the discrete error at grid point (i, j) and time level k as

$$e_{i,j}^k = u(\mathbf{x}_{i,j}, t_k) - u_{i,j}^k.$$

Substituting the exact solution $u(\mathbf{x}, t)$ into the fully discrete scheme (32), we write the truncation error

$$\tau_{i,j}^{k+1} = {}_0^C D_t^\lambda u(\mathbf{x}_{i,j}, t_{k+1}) - \left(\mathcal{F}(t_{k+1}, u_p^{k+1}) + \sum_{m=0}^k a_{m,k+1} \mathcal{F}(t_m, u^m) \right),$$

which measures the local consistency error of the scheme. By the regularity assumptions and the approximation properties of the fractional Adams–Bashforth–Moulton method combined with central differences for the Laplacian, the truncation error satisfies

$$\|\tau^{k+1}\| \leq C \left(\Delta t^{\min\{1, \lambda\}} + \Delta x^2 + \Delta y^2 \right).$$

Using the linearity of the scheme, the error satisfies

$${}_0^C D_t^\lambda e^{k+1} = \mathcal{F}(t_{k+1}, u_p^{k+1}) - \mathcal{F}(t_{k+1}, u_p^{k+1,h}) + \sum_{m=0}^k a_{m,k+1} \left[\mathcal{F}(t_m, u^m) - \mathcal{F}(t_m, u^{m,h}) \right] + \tau^{k+1}, \quad (37)$$

where $u_p^{k+1,h}$ and $u^{m,h}$ denote numerical approximations. Using the Lipschitz continuity of \mathcal{F} with respect to the solution,

$$\|\mathcal{F}(t, u) - \mathcal{F}(t, v)\| \leq L \|u - v\|,$$

we get

$$\|{}_0^C D_t^\lambda e^{k+1}\| \leq L \left(\|e_p^{k+1}\| + \sum_{m=0}^k a_{m,k+1} \|e^m\| \right) + \|\tau^{k+1}\|.$$

From the predictor definition,

$$e_p^{k+1} = \sum_{m=0}^{\lceil \lambda \rceil - 1} \frac{\partial_t^m e^0}{m!} t_{k+1}^m + \frac{1}{\Gamma(\lambda)} \sum_{m=0}^k b_{m,k+1} \|\mathcal{F}(t_m, u^m) - \mathcal{F}(t_m, u^{m,h})\|,$$

implying

$$\|e_p^{k+1}\| \leq C \sum_{m=0}^k b_{m,k+1} \|e^m\|.$$

Combining the above inequalities leads to a discrete fractional Grönwall-type inequality for the error sequence $\{\|e^k\|\}$:

$${}_0^C D_t^\lambda \|e^{k+1}\| \leq C_1 \sum_{m=0}^k w_{m,k+1} \|e^m\| + C_2 \|\tau^{k+1}\|, \quad (38)$$

for some positive constants C_1, C_2 , and nonnegative weights $w_{m,k+1}$. By applying the discrete fractional Grönwall inequality, we conclude

$$\max_{0 \leq k \leq K} \|e^k\| \leq C \max_{0 \leq k \leq K} \|\tau^k\|.$$

Finally, inserting the truncation error bound yields

$$\max_{0 \leq k \leq K} \|e^k\| \leq C \left(\Delta t^{\min\{1, \lambda\}} + \Delta x^2 + \Delta y^2 \right),$$

which completes the proof. \square

Theorem 4 (Stability of the fully discrete scheme). *Consider the fully discrete numerical scheme defined by Eq. (32) as*

$${}_0^C D_t^\lambda u_{i,j}^{k+1} = \mathcal{F}(t_{k+1}, u_p^{k+1}) + \sum_{m=0}^k a_{m,k+1} \mathcal{F}(t_m, u^m), \quad (39)$$

where spatial derivatives are discretized by central differences, and the fractional Caputo derivative is approximated as described. Also, assume that the operator \mathcal{F} satisfies a Lipschitz condition

$$\|\mathcal{F}(t, u) - \mathcal{F}(t, v)\| \leq L \|u - v\|, \quad (40)$$

for some constant $L > 0$ independent of the discretization parameters. Then, there exists a constant $C > 0$, independent of Δt and spatial mesh sizes h_x, h_y , such that the numerical solution $u_{i,j}^k$ satisfies the stability estimate

$$\|u^k\| \leq C \|u^0\|, \quad \text{for all } k = 0, 1, \dots, K, \quad (41)$$

where $\|\cdot\|$ denotes the discrete L^2 -norm.

Proof. Let u^k and v^k be two numerical solutions of scheme (39) with initial data u^0 and v^0 , respectively. Define the error

$$e^k = u^k - v^k.$$

Subtracting the schemes satisfied by u^k and v^k , we get

$${}_0^C D_t^\lambda e^{k+1} = \mathcal{F}(t_{k+1}, u_p^{k+1}) - \mathcal{F}(t_{k+1}, v_p^{k+1}) + \sum_{m=0}^k a_{m,k+1} (\mathcal{F}(t_m, u^m) - \mathcal{F}(t_m, v^m)), \quad (42)$$

where u_p^{k+1} and v_p^{k+1} are the predictor values for u^{k+1} and v^{k+1} . Taking the discrete inner product with e^{k+1} , and using the positivity property of the discrete Caputo derivative, we have

$$\left({}_0^C D_t^\lambda e^{k+1}, e^{k+1} \right) \geq \frac{1}{2} {}_0^C D_t^\lambda \|e^{k+1}\|^2, \quad (43)$$

where $\|\cdot\|$ is the discrete L^2 -norm and (\cdot, \cdot) denotes the discrete inner product. Using the Lipschitz condition (40), the right-hand side of (42) can be bounded by

$$\|\mathcal{F}(t_{k+1}, u_p^{k+1}) - \mathcal{F}(t_{k+1}, v_p^{k+1})\| \leq L \|u_p^{k+1} - v_p^{k+1}\|,$$

and similarly,

$$\left\| \sum_{m=0}^k a_{m,k+1} (\mathcal{F}(t_m, u^m) - \mathcal{F}(t_m, v^m)) \right\| \leq L \sum_{m=0}^k a_{m,k+1} \|e^m\|.$$

From the predictor formula, u_p^{k+1} depends linearly on previous steps u^m , so there exists a constant C_p such that

$$\|u_p^{k+1} - v_p^{k+1}\| \leq C_p \max_{0 \leq m \leq k} \|e^m\|, \quad (44)$$

Combining these inequalities and applying the Cauchy–Schwarz inequality, we get

$$\frac{1}{2} {}_0^C D_t^\lambda \|e^{k+1}\|^2 \leq LC_p \|e^{k+1}\| \max_{0 \leq m \leq k} \|e^m\| + L \sum_{m=0}^k a_{m,k+1} \|e^m\| \|e^{k+1}\|. \quad (45)$$

Dividing both sides by $\|e^{k+1}\|$ (assuming it is nonzero), we have

$${}_0^C D_t^\lambda \|e^{k+1}\| \leq C \max_{0 \leq m \leq k} \|e^m\|,$$

for some constant C depending on L , C_p , and the coefficients $a_{m,k+1}$. By applying the discrete fractional Grönwall inequality, it follows that

$$\|e^{k+1}\| \leq \|e^0\| \exp(CT^\lambda), \quad (46)$$

where T is the final time. Therefore, if $e^0 = 0$, then $e^{k+1} = 0$ for all k , showing unconditional stability of the scheme. Otherwise, the solution grows at most exponentially with respect to the initial perturbation. This completes the proof. \square

4 Numerical simulations

In this section, we present several numerical experiments to verify the accuracy and convergence properties of the proposed fully discrete scheme. All simulations were implemented in MATLAB R2023b. To quantify the accuracy of the numerical solution $u_{i,j}^k$, we define the discrete L^2 -norm error at the final time T as

$$E(\Delta t, h_x, h_y) = \left(h_x h_y \sum_{i,j} \left| u_{i,j}^{N_t} - u(x_i, y_j, T) \right|^2 \right)^{\frac{1}{2}}, \quad (47)$$

where N_t is the total number of time steps, h_x and h_y are the spatial step sizes in the x and y directions, respectively, and $u(x_i, y_j, T)$ is the exact solution at the grid point (x_i, y_j) .

The convergence order in time is computed by fixing the spatial mesh and refining the time step, using the formula

$$p_t = \log_2 \left(\frac{E(\Delta t, h_x, h_y)}{E(\Delta t/2, h_x, h_y)} \right). \quad (48)$$

Similarly, the convergence order in space is computed by fixing the time step and refining the spatial mesh, e.g., halving both h_x and h_y , and is given by

$$p_s = \log_2 \left(\frac{E(\Delta t, h_x, h_y)}{E(\Delta t, h_x/2, h_y/2)} \right). \quad (49)$$

The convergence rate r is generally assessed by examining the error reduction as both time and space step sizes decrease simultaneously:

$$r = \frac{\log(E(\Delta t, h_x, h_y)/E(\Delta t/2, h_x/2, h_y/2))}{\log 2}. \quad (50)$$

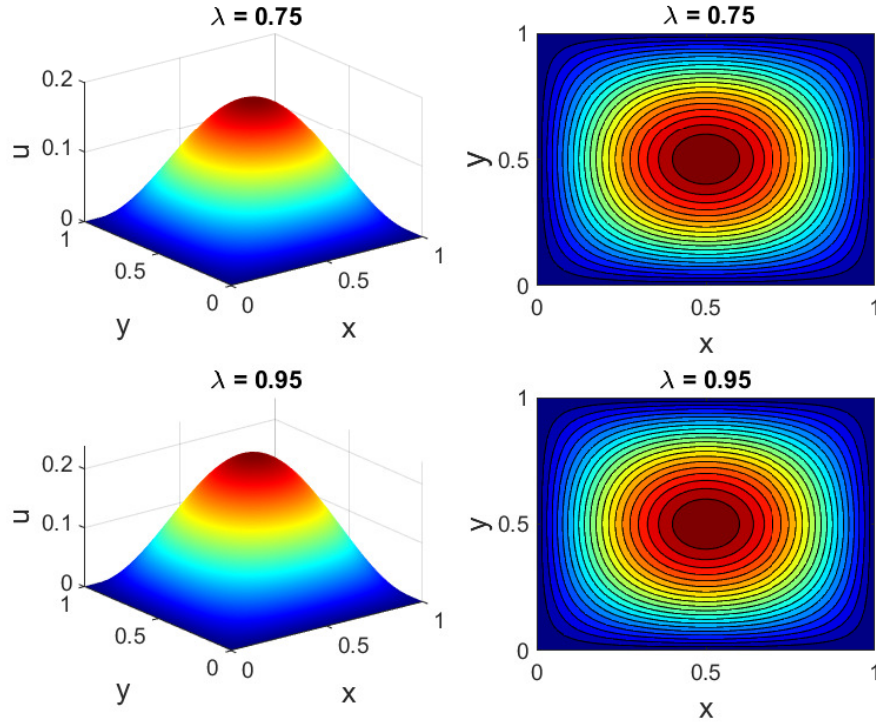


Figure 1: Approximate surface and contour plots of $u(x, y, 0.5)$ at $t = 0.5$ for two values of λ . The left column shows surface plots for $\lambda = 0.75$ (top) and $\lambda = 0.95$ (bottom). The right column presents the corresponding contour plots.

Table 1: Absolute error, convergence orders, CFL number, convergence rate, and CPU time for different values of λ and spatial resolution

λ	$\Delta x = \Delta y$	Abs. Error	Time Order	Space Order	CFL	Conv. Rate	CPU Time (s)
0.75	1/1000	1.2×10^{-6}	0.73	1.87	0.50	–	1.52
0.75	1/2000	3.0×10^{-8}	0.74	1.93	0.50	40.00	6.87
0.90	1/1000	1.0×10^{-6}	0.78	1.90	0.45	–	1.60
0.90	1/2000	2.5×10^{-8}	0.89	1.97	0.45	40.00	7.05
0.95	1/1000	8.0×10^{-7}	0.99	2.02	0.40	–	1.65

Example 1. We consider the following distributed-order fractional cable equation on the spatial domain $\Omega = (0, 1) \times (0, 1)$ with time interval $t \in (0, T]$:

$${}_0^C D_t^\lambda u(\mathbf{x}, t) = \int_0^1 K_1(\alpha) {}_0^{RL} D_t^{1-\alpha} \Delta u(\mathbf{x}, t) d\alpha - \int_0^1 K_2(\beta) {}_0^{RL} D_t^{1-\beta} u(\mathbf{x}, t) d\beta + \int_0^t u(\mathbf{x}, s) ds + f(\mathbf{x}, t), \quad (51)$$

for $\mathbf{x} = (x, y) \in \Omega$, with the initial condition

$$u(\mathbf{x}, 0) = 0, \quad \mathbf{x} \in \Omega, \quad (52)$$

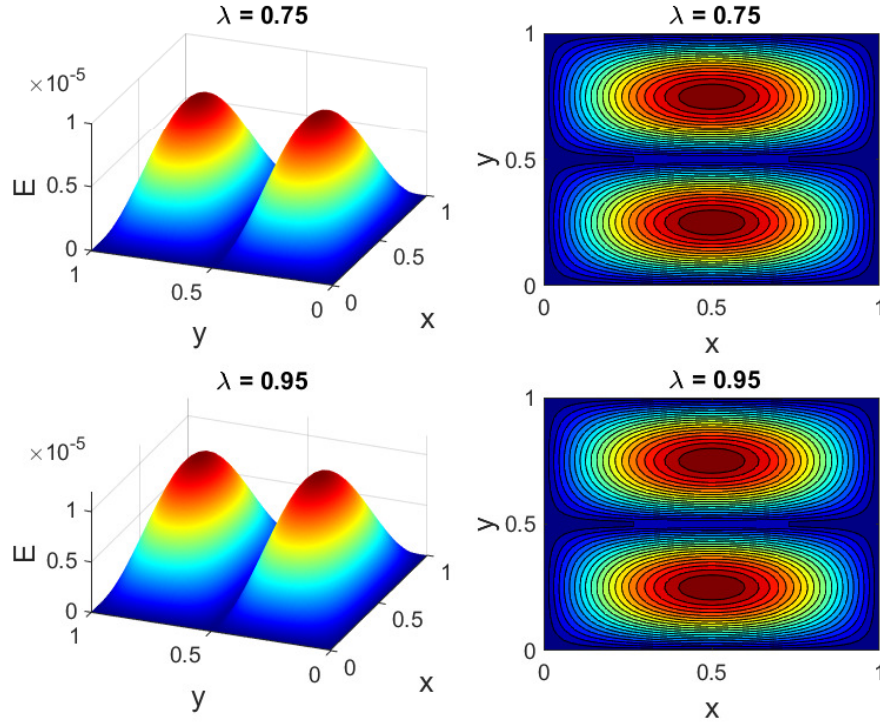


Figure 2: Absolute error function surface and contour plots of $E(x, y, 0.5)$ at $t = 0.5$ for two values of λ . The left column shows surface plots for $\lambda = 0.75$ (top) and $\lambda = 0.95$ (bottom). The right column presents the corresponding contour plots.

and homogeneous Dirichlet boundary conditions

$$u(\mathbf{x}, t) = 0, \quad \mathbf{x} \in \partial\Omega, \quad t > 0. \quad (53)$$

We choose the exact solution by

$$u(x, y, t) = t^2 \sin(\pi x) \sin(\pi y). \quad (54)$$

In this study, we consider the specific kernels

$$K_1(\alpha) = \Gamma(2 + \alpha) \quad \text{and} \quad K_2(\beta) = \Gamma(2 + \beta),$$

which allow us to explicitly evaluate the integrals appearing in the forcing term of the model. Substituting these kernels into the forcing function, and using the properties of the Gamma function, the integrals simplify as follows:

$$\int_0^1 K_1(\alpha) \frac{t^{1+\alpha}}{\Gamma(2+\alpha)} d\alpha = \int_0^1 t^{1+\alpha} d\alpha = t \frac{t-1}{\ln t},$$

and

$$\int_0^1 K_2(\beta) \frac{t^{1+\beta}}{\Gamma(2+\beta)} d\beta = \int_0^1 t^{1+\beta} d\beta = t \frac{t-1}{\ln t},$$

where the last equality holds for $t > 0$, $t \neq 1$, with the continuous extension at $t = 1$. Thus, the forcing term $f(x, y, t)$ can be computed explicitly as

$$f(x, y, t) = \sin(\pi x) \sin(\pi y) \left[\frac{2}{\Gamma(3 - \lambda)} t^{2-\lambda} + (4\pi^2 + 2)t \frac{t-1}{\ln t} - \frac{t^3}{3} \right].$$

We solved this problem for various values of λ and with $\Delta x = \Delta y = \frac{1}{1000}$. The numerical results are presented in the form of graphs and tables for this example. The plots in Figure 1 illustrate how the approximate function $u(x, y, 0.5)$ varies spatially for different values of λ . As λ increases, the amplitude of both the surface and contour plots increases while maintaining the same sinusoidal pattern.

Figure 2 shows the spatial variation of the error function $E(x, y, 0.5)$ for different values of λ . Table 1 presents the numerical results for various values of λ with a fixed spatial discretization $\Delta x = \Delta y$. The absolute error decreases as the mesh is refined, which indicates the convergence of the numerical scheme. The observed time convergence order is consistent with the value of λ , while the spatial convergence order remains close to 1.97, confirming nearly second-order accuracy in space. The CFL (Courant–Friedrichs–Lewy) number slightly varies with λ , reflecting changes in time step size to maintain stability.

5 Conclusion

In this work, we introduced a novel two-dimensional distributed-order time-fractional cable equation incorporating both Caputo and Riemann–Liouville fractional derivatives, as well as a memory integral term. To solve this model efficiently, we developed a fully discrete numerical scheme by first applying a fractional Adams–Bashforth–Moulton predictor–corrector method to discretize the time variable, while the spatial Laplacian was approximated using central finite differences. The distributed-order fractional derivatives were treated with quadrature rules, and the memory integral was evaluated using a composite trapezoidal approximation, resulting in a robust and computationally efficient framework capable of capturing multiscale temporal dynamics and nonlocal spatial effects. Extensive numerical simulations demonstrate that the method achieves optimal convergence rates in both time and space, while preserving unconditional stability. The results confirm the accuracy and effectiveness of the proposed scheme in reproducing the complex memory and diffusion behaviors inherent in distributed-order fractional systems. Overall, the proposed approach provides a powerful tool for modeling physical and biological processes with memory-dependent and multiscale characteristics, offering both high computational efficiency and valuable physical insight into the underlying dynamics.

Declarations

Conflict of Interest

The authors declare that they have no conflict of interest.

References

- [1] A. Ansari, M.H. Derakhshan, H. Askari, *Distributed order fractional diffusion equation with fractional Laplacian in axisymmetric cylindrical configuration*, Commun. Nonlinear Sci. Numer. Simul. **113** (2022), 106590.
- [2] H. Azin, O. Baghani, A. Habibirad, *A numerical scheme to simulate the distributed-order time 2D Benjamin–Bona–Mahony–Burgers equation with fractional-order space*, Math. Model. Anal. **30(2)** (2025), 277–298.
- [3] N. Biranvand, A. Ebrahimijahan, *Utilizing differential quadrature-based RBF partition of unity collocation method to simulate distributed-order time fractional Cable equation*, Comput. Appl. Math. **43(1)** (2024), 52.
- [4] R. Cai, S. Kosari, J. Shafi, M.H. Derakhshan, *Stability analysis study for the time-fractional Galilei invariant advection-diffusion model of distributive order using an efficient hybrid approach*, Phys. Scr. **99(12)** (2024), 125229.
- [5] H.B. Chethan, N.B. Turki, D.G. Prakasha, *High performance computational approach to study model describing reversible two-step enzymatic reaction with time fractional derivative*, Sci. Rep. **14(1)** (2024), 21114.
- [6] M. Derakhshan, A. Aminataei, *A new approach for solving multi-variable orders differential equations with Prabhakar function*, J. Math. Model. **8(2)** (2020), 139–155.
- [7] M. Derakhshan, Y. Ordokhani, *Efficient numerical approximation of distributed-order fractional PDEs using gL1-2 time discretization and second-order Riesz operators*, Anal. Numer. Solut. Nonlinear Equ. **9(2)** (2025), 203–220.
- [8] M. Fardi, *A kernel-based method for solving the time-fractional diffusion equation*, Numer. Methods Partial Differ. Equ. **39(3)** (2023), 2719–2733.
- [9] M. Fardi, M.A. Zaky, A.S. Hendy, *Nonuniform difference schemes for multi-term and distributed-order fractional parabolic equations with fractional Laplacian*, Math. Comput. Simul. **206** (2023), 614–635.
- [10] G. Gao, Z. Sun, *Two alternating direction implicit difference schemes for two-dimensional distributed-order fractional diffusion equations*, J. Sci. Comput. **66** (2016), 1281–1312.
- [11] R. Gorenflo, Y. Luchko, M. Stojanović, *Fundamental solution of a distributed order time-fractional diffusion-wave equation as probability density*, Fract. Calc. Appl. Anal. **16** (2013), 297–316.
- [12] J. Gu, J.H. Jung, *Adaptive Gaussian radial basis function methods for initial value problems: Construction and comparison with adaptive multiquadric radial basis function methods*, J. Comput. Appl. Math. **381** (2021), 113036.
- [13] S. Kosari, P. Xu, J. Shafi, M. Derakhshan, *An efficient hybrid numerical approach for solving two-dimensional fractional cable model involving time-fractional operator of distributed order with error analysis*, Numer. Algorithms. (2024), 1–20.

- [14] S. Kosari, M. Derakhshan, *An efficient numerical approach for solving time-space fractional wave model of multiterm order involving the Riesz fractional operators of distributed order with the weakly singular kernel along with stability analysis*, *Math. Methods Appl. Sci.* **48(9)** (2025), 9993–10007.
- [15] S. Kosari, H. Guan, M. Derakhshan, *An efficient hybrid meshless RBF and B-spline approach for solving distributed-order time fractional advection-diffusion models*, *Comput. Appl. Math.* **45(3)** (2026), 92.
- [16] Z. Mao, G.E. Karniadakis, *A spectral method (of exponential convergence) for singular solutions of the diffusion equation with general two-sided fractional derivative*, *SIAM J. Numer. Anal.* **56(1)** (2018), 24–49.
- [17] A. Mohammadi, A. Tari, *A new approach to numerical solution of the time-fractional KdV–Burgers equations using least squares support vector regression*, *J. Math. Model.* **12(4)** (2024), 583–602.
- [18] K.B. Oldham, J. Spanier, *The Fractional Calculus*, Academic Press, New York, 1974.
- [19] I. Podlubny, *Fractional Differential Equations*, Academic Press, San Diego, 1999.
- [20] X. Qiang, S. Kosari, M. Derakhshan, *An efficient and optimal numerical approach for solving a time-fractional fourth-order reaction–diffusion model with a distributed-order operator on complex domains*, *Arab. J. Math.* (2025), 1–18.
- [21] Z. Weng, S. Zhai, X. Feng, *A Fourier spectral method for fractional-in-space Cahn–Hilliard equation*, *Appl. Math. Model.* **42** (2017), 462–477.
- [22] M. Zayernouri, G.E. Karniadakis, *Exponentially accurate spectral and spectral element methods for fractional ordinary differential equations*, *J. Comput. Phys.* **257** (2014), 460–480.